PHYSICAL REVIEW A VOLUME 24, NUMBER 6 DECEMBER 1981

Semiclassical theory of rotationally induced nonadiabatic transitions

Hiroki Nakamura*
Engineering Science Laboratory, Faculty of Technology, Tokyo University of Agriculture and Technology, Koganei, Tokyo 184, Japan

Masatoshi Namiki
Physics Laboratory, Division of General Education, Takachiho College, 2-19-1 Ohmiya, Suginami-ku, Tokyo 168, Japan
(Received 1 June 1981)

A general procedure is proposed to treat a many-state atomic-collision problem involving both nonadiabatic radial and rotational couplings. The procedure is based on the classical S-matrix theory in a new "dynamical-state" representation. The dynamical states are defined as the eigenstates of a new Hamiltonian operator which is composed of an ordinary electronic Hamiltonian and a Coriolis coupling term. The dynamical potential energies thus obtained avoid crossings even for the rotationally coupled states. At these avoided crossing points the rotationally induced transitions predominantly occur, which are delocalized in the ordinary adiabatic-state representation. The theory is applied to certain two-state- and three-state-model problems, and is shown to work well. An interesting catalytic phenomenon is found in a three-state problem. A certain transition is enhanced by a rotational coupling not directly associated with that transition; besides, a transition directly induced by that rotational coupling is not affected by the coupling responsible for the first transition. This phenomenon can be successfully explained and reproduced by the theory. A condition is discussed for this kind of phenomenon to occur in a general many-state collision problem involving rotational couplings.

I. INTRODUCTION

Among a variety of mechanisms the following four represent the basic ones which govern the various atomic and molecular dynamic processes: (1) electron correlation (configuration interaction), (2) nonadiabatic radial coupling, (3) diabatic coupling between molecular Rydberg states, and (4) nonadiabatic rotational coupling. The first one is the mechanism responsible for the decay of molecular-resonance states embedded in the electronic continuum. Penning ionization and a unimolecular decay of the superexcited states are the typical examples of the relevant dynamic processes.[1,2] These processes can be treated, to a good accuracy, by the local complex potential method. The nonadiabatic radial coupling represents the best known mechanism which is responsible for the transitions between low-lying excited-adiabatic-molecular states of the same symmetry. The transition is well localized at an avoided crossing of potential-energy curves. As is well known, the Landau-Zener-Stueckelberg (LZS) theory, and its extensions and modifications can be successfully applied to the problem.[3] If we use the ordinary adiabatic-state representation, the transitions involving molecular Rydberg states are also governed by the nonadiabatic radial coupling. The treatment on this line, however, is not very efficient, since no avoided crossing exists between the Rydberg states. A more elegant way of treating the problem is given by the multichannel quantum-defect theory (MQDT).[4,5] Determination of energy levels of the perturbed Rydberg states,[5] autoionization of vibrationally and/or rotationally excited Rydberg states,[6,7] and the dissociative recombination involving Rydberg states as intermediate ones[8] have been quite successfully treated by MQDT. The theory seems prospective for an extensive use in the studies of various atomic-collision processes.[9]

Rotational coupling presents another important nonadiabatic coupling which governs a transition between the adiabatic states of different symmetry.

This coupling is known to play a decisive role in high-energy ion-atom collisions.[10] In general, however, the rotational coupling has been given less attention compared to the radial coupling. For instance, its role in chemical reaction systems should be more carefully investigated. Also an effort should be paid more to derive analytical formulas for the amplitude of a transition induced by this coupling. It is desirable to develop a theory which not only gives a useful analytical expression for the transition amplitude, but also makes the transition localized at a certain point such as a pseudocrossing point in the radial coupling problem. The localization of the transition is important, since it would enable us to deal with a many-state collision problem by a step-by-step treatment based on the two-state collision theory. A theory which meets these requirements was proposed recently[11] by using the dynamical-potential representation.[12] The theory was tested to work quite well in two-state problems.

In Sec. II of this paper an analytical structure of rotational coupling problems is reviewed in comparison with that of the radial coupling problems. The dynamical-state representation is introduced in Sec. III. The new representation tranforms the analytical structure into the one the same as that of the radial coupling problems, and thus enables us to employ the conventional Landau-Zener-Stueckelberg or Rozen-Zener (RZ) formulas. Section IV demonstrates the usefulness of the theory in the basic two-state problems. By merging the theory into the path-integral formulation of a scattering matrix,[13] an application is also made in Sec. V to a three-state problem which imitates a vacancy migration from the $2p$-shell to the $2s$ or $1s$ shell in the Ne^+-Ne system. This system involves two rotational couplings: one between the $1\pi_u$ and $2\sigma_u$ states, and the other between the $1\pi_u$ and $1\sigma_u$ states. The problem is shown to be successfully treated by the path-integral formulation based on the new dynamical potentials. The new potentials are obtained by diagonalizing the 3×3 matrix, the diagonal elements of which are the ordinary adiabatic energies, and the off-diagonal elements of which are the rotational coupling terms. An interesting catalysis effect of the $2\sigma_u$ state on the transition $1\pi_u \rightarrow 1\sigma_u$ was found. This effect can be reproduced well by the classical S-matrix theory based on the dynamical potentials. A prescription is discussed to treat a general many-state collision problem involving both rotational and radial couplings. For simplicity the linear-trajectory-impact-parameter method is employed throughout the paper. Thus the internuclear distance R is given as

$$R^2=\rho^2+v^2t^2 ,$$

where ρ is the impact parameter, v the collision velocity, and t is time. Atomic units are used throughout the paper.

II. ANALYTICAL PROPERTIES OF NONADIABATIC ROTATIONAL COUPLING

As is well known, the complex zero $R_*=R(t_*)$ of the difference $\Delta\epsilon(R)$ of adiabatic potential energies play an important role in the nonadiabatic transitons induced by radial coupling. The real part of R_* is roughly equal to the avoided crossing point where $|\Delta\epsilon|$ becomes minimum on the real axis of R. Since R as a complex variable can be expanded in a Taylor series at $t=t_*$,

$$R\simeq R_*+\left[\frac{dR}{dt}\right]_{t_*}(t-t_*)+\cdots , \tag{1}$$

and $\Delta\epsilon(R)$ is proportional to $(R-R_*)^{1/2}$ around $R=R_*$, the zero of $\Delta\epsilon(R)$ is of the order one-half with respect to t,

$$\Delta\epsilon(R)\propto(t-t_*)^{1/2} \text{ for } t\sim t_* . \tag{2}$$

The nonadiabatic radial coupling V_{rad} can be shown to have a pole of order unity there,[14]

$$V_{\text{rad}}=\dot{R}\left\langle\varphi_1\left|\frac{\partial\varphi_2}{\partial R}\right\rangle\right.\simeq\frac{i}{4}(t-t_*)^{-1} , \tag{3}$$

where φ_j $(j=1,2)$ are the electronic eigenfunctions of adiabatic states. This analytical property underlies the derivation of the closed expressions for the scattering matrix,[12,15] namely, the Landau-Zener-Stueckelberg formula and the Rozen-Zener (or the Demkov) formula. Basic differential equations to describe these two cases can be reduced to an equation satisfied by the parabolic-cylinder (Weber) functions. The comparison equation method[16–18] and the Zwaan-Stueckelberg phase-integral method[12] are the fundamental mathematics employed to derive these analytical formulas. The apparent difference in these two (LZS and RZ) formulas comes from the difference in the asymptotic expressions of the Weber functions.

In the case of nonadiabatic transitions induced by rotational coupling, the following three cases are considered to be the basic two-state problems:

(a) potential curve crossing at the finite internuclear distance ($R=R_x$), (b) degeneracy at the united-atom limit ($R=0$), and (c) no curve crossing. In case (a) there exists a real curve crossing at $R_x=R(t_x)$, and $\Delta\epsilon$ has a zero of order unity with respect to t at $t=t_x$. In case (b) $\Delta\epsilon(R)$ can usually be approximated as

$$\Delta\epsilon(R)\propto R^2 \text{ for } R\sim 0 . \tag{4}$$

Since R^2 (not R itself) is an analytical function of t^2 around $t=t_c$ where $R(t_c)=0$, R cannot be expanded in a Taylor series there, but is proportional to $(t-t_c)^{1/2}$. Thus $\Delta\epsilon$ has a zero of order unity with respect to t at $t=t_c$. The simplest model to case (c) is constant energy difference ($\Delta\epsilon=$const), for which no zero exists. On the other hand, irrespective of functional form of $\Delta\epsilon(R)$, the rotational coupling term $V_{\rm rot}$ [see Eq. (17)] has a pole of order unity with respect to t at $t=t_c$, since $R\propto(t-t_c)^{1/2}$ at $t\simeq t_c$. The analytical properties mentioned above are summarized in Table I. So far, the above three cases (a)–(c) have been discussed separately because of the difference in the analytical properties.[15,19,20] It is desirable to develop a theory which can handle all the cases at the same time in a unified way. Throughout this paper the electronic angular momentum matrix element V_0 [see Eq. (17)] is assumed to be constant. In reality V_0 is, of course, generally a function of R. If V_0 vanishes faster than R^2 when $R\rightarrow 0$, then the pole of $V_{\rm rot}$ at $t=t_c$ becomes a removable singularity. As explained below, however, the essential qualitative features of the theory developed in this paper would remain unchanged even with an R dependent V_0.

III. DYNAMICAL-STATE REPRESENTATION

Expanding the total wave function Ψ of the system in terms of a certain orthonormal complete set of basis functions $\{\psi_j\}$,

$$\Psi=\sum_j A_j(t)\psi_j(\vec{r};R), \tag{5}$$

and inserting this expansion into the time-dependent Schrödinger equation

$$i\hbar\frac{\partial\Psi}{\partial t}=\hat{H}_{\rm el}\Psi, \tag{6}$$

we have the following coupled differential equations:

$$i\hbar\frac{dA_k}{dt}=\sum_j\langle\psi_k\mid\hat{H}_{\rm el}\mid\psi_j\rangle_{\vec{r}}A_j - i\hbar\sum_j\left\langle\psi_k\left|\frac{\partial\psi_j}{\partial t}\right.\right\rangle_{\vec{r}}A_j. \tag{7}$$

TABLE I. Analytical properties of nonadiabatic couplings.

Coupling scheme	Potential-energy difference	Coupling term
Radial:		
$R-R_*\propto(t-t_*)$	$\Delta\epsilon\propto(t-t_*)^{1/2}$	$V_{\rm rad}\propto(t-t_*)^{-1}$
t_*, R_* : complex		
Rotational: case (a)		
$R-R_x\propto(t-t_x)$		
$R\propto(t-t_c)^{1/2}$	$\Delta\epsilon\propto(t-t_x)$	$V_{\rm rot}\propto(t-t_c)^{-1}$
t_x: real, t_c; complex		
Rotational: case (b)		
$R\propto(t-t_c)^{1/2}$	$\Delta\epsilon\propto(t-t_c)$	$V_{\rm rot}\propto(t-t_c)^{-1}$
t_c: complex		
Rotational: case (c)		
$R\propto(t-t_c)^{1/2}$	$\Delta\epsilon$: const	$V_{\rm rot}\propto(t-t_c)^{-1}$
t_c: complex		
Rotational: dynamical-state representation		
[see Eqs. (18) and (19)]	$\Delta E\propto(t-t_*)^{1/2}$	$W\propto(t-t_*)^{-1}$
$R-R_*\propto(t-t_*)$		
t_*, R_*: complex		

Here $\vec{r}$ represents the totality of electron coordinates, $\hat{H}_{el}$ is the electronic Hamiltonian of the system. If ψ_j's are the eigenfunctions of $\hat{H}_{el}$, then Eqs. (7) give the conventional coupled equations in the adiabatic-state representation. If we use a transformation,

$$\frac{\partial}{\partial t}=\dot{R}\frac{\partial}{\partial R}+\frac{i}{\hbar}\dot{\Theta}\left[-i\hbar\frac{\partial}{\partial\Theta}\right]$$
$$=\dot{R}\frac{\partial}{\partial R}-\frac{i}{\hbar}\dot{\Theta}\hat{L}_x, \tag{8}$$

we can rewrite Eqs. (7) as

$$\frac{dA_k}{dt}=-\sum_j\dot{R}\left\langle\psi_k\left|\frac{\partial\psi_j}{\partial R}\right.\right\rangle_{\vec{r}}A_j$$
$$-\frac{i}{\hbar}\sum_j\langle\psi_k\,|\,\hat{H}_{el}-\dot{\Theta}\hat{L}_x\,|\,\psi_j\rangle_{\vec{r}}A_j, \tag{9}$$

where $\dot{\Theta}$ is the angular velocity of the internuclear axis, $\hat{L}_x$ is that component of the electronic angular momentum operator which is perpendicular to the plane of the collision trajectory (see Fig. 1). These quantities are explicitly defined as

$$\dot{\Theta}=v\rho/R^2 \tag{10}$$

and

$$\hat{L}_x=\tfrac{1}{2}(\hat{L}_+ +\hat{L}_-), \tag{11}$$

where $\hat{L}_+$ and $\hat{L}_-$ denote the raising and lowering operators for azimuthal angular momentum along the internuclear axis.

If we assume that ψ_j's are the eigenfunctions of $\hat{H}_{el}-\dot{\Theta}\hat{L}_x$, i.e.,

$$\hat{H}_{dyn}\psi_j\equiv(\hat{H}_{el}-\dot{\Theta}\hat{L}_x)\psi_j=E_j(R)\psi_j, \tag{12}$$

then we have from Eq. (9)

$$\frac{dA_k}{dt}=-\frac{i}{\hbar}E_k(R)A_k-\sum_{j\neq k}\dot{R}\left\langle\psi_k\left|\frac{\partial\psi_j}{\partial R}\right.\right\rangle_{\vec{r}}A_j. \tag{13}$$

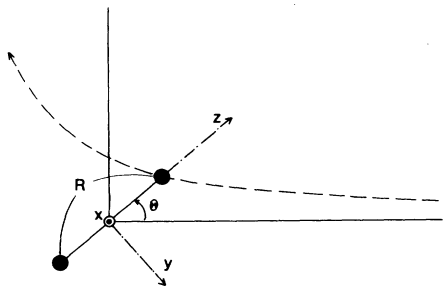

FIG. 1. Geometry of the collision system.

Since the operator on the left-hand side of Eq. (12) is Hermitian, the eigenvalues $E_j(R)$ are real. Equations (13) have exactly the same form as the equations obtained in the radial coupling problems based on the ordinary adiabatic-state representation. Since the nuclear angular motion is incorporated in the basis functions ψ_j of Eq. (12), we call the new states "dynamical" states. In this new representation eigenstates of $\hat{H}_{el}$ (ordinary adiabatic states) play, in a sense, a role of the conventional diabatic states, and ψ_j's play a role of the conventional adiabatic states. The new energies and couplings can be shown to have the same analytical structures as those in the conventional radial coupling problems [see Eqs. (18) and (19), and Table I]. If the collision system we are interested in is composed only of the states of the same symmetry, then there is no rotational coupling and the eigenvalue problem (12) simply reduces to the ordinary eigenvalue problem of determining the adiabatic energies for which the noncrossing rule holds. If there are the states of different symmetry with real curve crossings, then the dynamical states obtained as the solutions of Eq. (12) avoid the crossings (Fig. 2). Thus the dynamical-state representation enables us to apply the LZS and RZ theories to a general collision problem involving both radial and rotational couplings. This representation makes all the (rotational as well as radial) transitions localized at the complex crossing points of the dynamical potentials.

In order to look into the new representation more explicitly, let us consider the simplest case of a two (Σ and Π)-state problem. Let ϵ_Λ and φ_Λ be the adiabatic energies and eigenfunctions, i.e.,

$$\hat{H}_{el}\varphi_\Lambda=\epsilon_\Lambda\varphi_\Lambda \quad (\Lambda=\Sigma,\Pi). \tag{14}$$

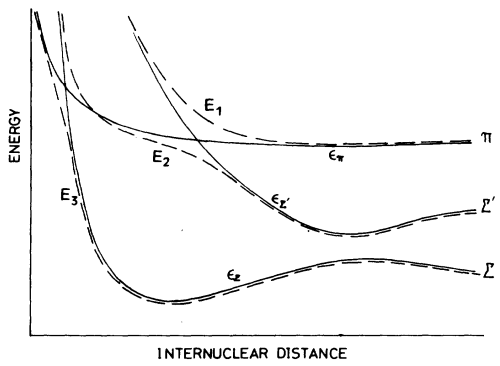

FIG. 2. Schematic diagram of adiabatic- and dynamical-potential energies. —— : adiabatic states ϵ_Λ, — — — : dynamical states E_j.

Expanding the dynamical eigenfunction ψ_j in terms of these adiabatic wave functions as

$$\psi_j = C_j^{\Sigma}\varphi_{\Sigma} + C_j^{\Pi}\varphi_{\Pi} \quad (j=1,2) \tag{15}$$

we obtain the following secular equations from Eq. (12):

$$(\epsilon_{\Sigma}-E)C^{\Sigma} + V_{\rm rot}C^{\Pi} = 0, \tag{16a}$$

$$V_{\rm rot}C^{\Sigma} + (\epsilon_{\Pi}-E)C^{\Pi} = 0, \tag{16b}$$

where

$$V_{\rm rot} = -\dot{\Theta}\langle\varphi_{\Sigma} \mid \hat{L}_x \mid \varphi_{\Pi}\rangle_{\vec{r}} \equiv -\frac{v\rho}{R^2}V_0. \tag{17}$$

From these equations we have as usual,

$$E_{1,2} = \tfrac{1}{2}\{\epsilon_{\Sigma}+\epsilon_{\Pi} \pm [(\Delta\epsilon)^2 + 4V_{\rm rot}^2]^{1/2}\}, \tag{18}$$

and

$$W \equiv \left\langle \psi_1 \left| \frac{\partial\psi_2}{\partial R} \right\rangle_{\vec{r}} \dot{R} = C_1^{\Sigma}\dot{C}_2^{\Sigma} + C_1^{\Pi}\dot{C}_2^{\Pi} \right.$$
$$= \left[\Delta\epsilon \frac{dV_{\rm rot}}{dt} - \frac{d\Delta\epsilon}{dt} V_{\rm rot} \right] \Big/ (\Delta E)^2, \tag{19}$$

where

$$\Delta\epsilon = \epsilon_{\Sigma} - \epsilon_{\Pi} \tag{20}$$

and

$$\Delta E = E_1 - E_2 = [(\Delta\epsilon)^2 + 4V_{\rm rot}^2]^{1/2}. \tag{21}$$

It should be noted that the difference of the dynamical-potential energies depends on the collision velocity as well as the impact parameter. The energies given by Eq. (18) corresponds to the "dynamical-adiabatic" representation proposed by Crothers.[12] A similar representation, angular diabatic representation, was discussed by Smith.[21] As mentioned before, we call here the states ψ_j dynamical states, since the potentials depend on the velocity, and the expression adiabatic is considered not to be pertinent. The energy difference ΔE and the coupling W can easily be proved to have the analytical structure shown in Table I irrespective of the functional forms of $\Delta\epsilon(R)$ [cases (a)–(c)]. These analytical properties of ΔE and W are not affected by a possible R dependence of V_0. Since a new coupling W is proportional to $(\Delta E)^{-2}$, W always has a pole at exactly the same position as the zero of ΔE.

In a general many-state collision problem, the dynamical states are obtained by diagonalizing a matrix $(\underline{\epsilon}+\underline{V}_{\rm rot})$, where $\underline{\epsilon}$ is a diagonal matrix whose elements are the ordinary adiabatic potential energies ϵ_i, and

$$(\underline{V}_{\rm rot})_{ij} = -\frac{v\rho}{R^2}\langle\varphi_i \mid \hat{L}_x \mid \varphi_j\rangle_{\vec{r}} \tag{22}$$

with

$$\hat{H}_{\rm el}\varphi_i = \epsilon_i\varphi_i.$$

By this diagonalization procedure the avoided crossings between the adiabatic states of the same symmetry remain avoided, and the real crossings between the adiabatic states of different symmetry become avoided (Fig. 2). Once we obtain a dynamical-potential-energy system, we can apply the path-integral formulation of the scattering matrix or the classical S-matrix theory,[13] assuming a localized transition at a new avoided crossing point. Localization of the transitions at the new avoided crossing points will be demonstrated in the subsequent sections. It is interesting to note that since rotational coupling is delocalized, even a rotational coupling not directly associated with a transition we are interested in, could largely affect that transition. This phenomenon would occur most effectively when an avoided crossing associated with the transition we are interested in is located at small internuclear distances. This is because a rotational coupling has always a pole at $R=0$ unless the angular momentum matrix element V_0 vanishes there. An example of this interesting phenomenon is shown in Sec. V.

IV. BASIC TWO-STATE PROBLEMS

In this section the theory developed in the previous section is applied to the typical two-state problems (a)–(c) mentioned before. The theory is tested by comparing the results on the transition probabilities and the cross sections with the exact ones obtained from a numerical solution of the coupled equations. Some of the results cited below were reported before. The analytical formulas employed to estimate the transition probabilities are

$$P_{\rm LZS}(v,\rho) = 4e^{-2\delta}(1-e^{-2\delta})\sin^2\phi, \tag{23}$$

and

$$P_{\rm RZ}(v,\rho) = \operatorname{sech}^2\delta\sin^2\sigma$$
$$= 4\frac{1}{1+e^{-2\delta}}\left[1-\frac{1}{1+e^{-2\delta}}\right]\sin^2\sigma, \tag{24}$$

where

$$\phi = \sigma + \phi_S, \tag{25}$$

$$\sigma+i\delta=\frac{1}{v}\int_0^{z_*}\Delta E dz,\quad z_*=vt_* \tag{26}$$

and

$$\phi_S=\frac{\pi}{4}-\frac{\delta}{\pi}+\left[\frac{\delta}{\pi}\right]\ln\left[\frac{\delta}{\pi}\right]-\arg\Gamma\left[1+i\frac{\delta}{\pi}\right]. \tag{27}$$

Here ΔE is the difference of the dynamical potentials [Eq. (21)] and t_* is the zero of ΔE closest to the real axis in the first quadrant of the complex t plane. The total cross section is calculated by

$$\sigma_t=2\pi\int_0^{\infty}d\rho\, P(v,\rho)\rho. \tag{28}$$

A. Curve crossing at the finite internuclear distance ($R=R_x$)—case (a)

The following model is used:

$$\Delta\epsilon=2.71(1/R_x-1/R)\quad R_x=1.5$$

and

$$V_0=0.71. \tag{29}$$

This simulates the two-state ($1\pi_u$ and $2\sigma_u$) problem in the Ne^+-Ne system.[19,22] Equation (23) was shown to well reproduce the impact-parameter dependence of the transition probabilities as well as the velocity dependence of the cross sections (see Fig. 1 and 2 of Ref. 11). Equation (24) is not a good approximation in this case. The transition mechanism is not that of the perturbed symmetric resonance. Figure 3 demonstrates how localized the transitions are. The step functions shown in the figures represent the approximation of the path-integral formulation based on the assumption of a localized transition at $R=\mathrm{Re}(R_*)$. The value of this step function in between the two points $R=\mathrm{Re}(R_*)$ (on the way in and on the way out) is simply equal to $\exp(-\delta)$, a transition probability for one passage of the avoided crossing point. The asymptotic value for $R>\mathrm{Re}(R_*)$ on the way out equals P_{LZS} given by Eq. (23), an overall transition probability after collision. This figure clearly indicates the effectiveness of the new representation compared to the ordinary adiabatic representation. At large impact parameters, however, the localization becomes somewhat worse. This is because the two pairs of transition points (one on the way in and one on the way out) come close to each other.

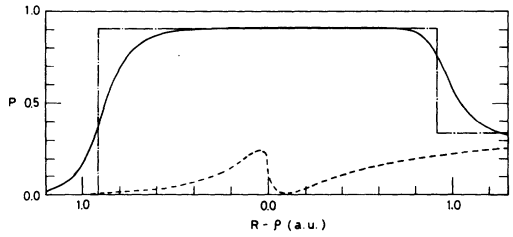

FIG. 3. Transition probabilities vs internuclear distance [model (29), $v=0.5$, $\rho=0.6$]. Left (right) of the point $R-\rho=0$ corresponds to the incoming (outgoing) channel. —— : exact numerical calculation based on the dynamical-state representation, — · — · —: LZS approximation based on the assumption of a localized transition at $R=\mathrm{Re}(R_*)$ [Eq. (23)], — — — : exact numerical calculation based on the adiabatic-state representation.

B. Degeneracy at the united-atom limit—case (b)

The model used here is

$$\Delta\epsilon=0.1Z_{\mathrm{eff}}^4R^2=536.9R^2,\quad Z_{\mathrm{eff}}=8.56$$

and

$$V_0=1.0. \tag{30}$$

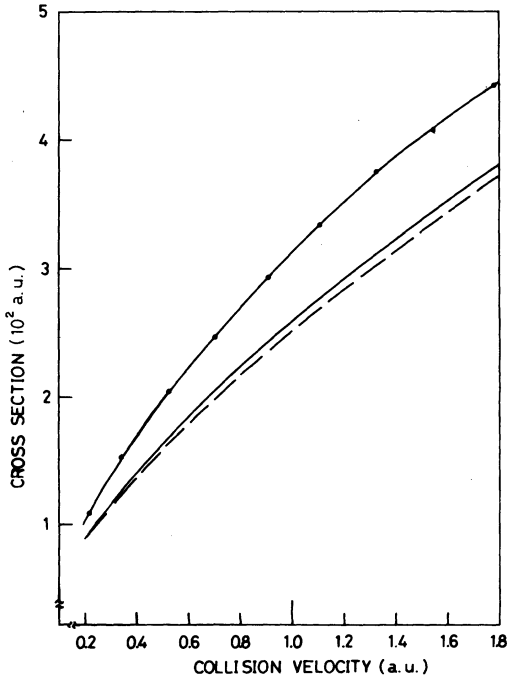

FIG. 4. Total cross sections as a function of collision velocity [model (30)]. —— : LZS approximation [Eq. (23)], — — — : exact numerical calculation, —o—o— : RZ approximation [Eq. (24)].

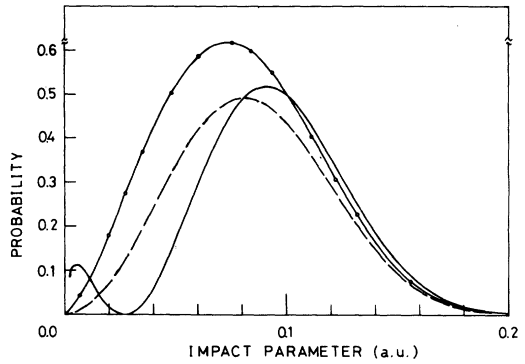

FIG. 5. The impact-parameter dependence of the transition probabilities [model (30), $v=0.9$]. The meanings of the curves are the same as Fig. 4.

This simulates the coupling between the $1\pi_u$ and $1\sigma_u$ states of the Ne^+-Ne system.[22,23] It should be noted that the linear-trajectory approximation is good only at high velocities ($v \gtrsim 0.5$). As is seen from Fig. 4 the total cross sections are reproduced well by Eq. (23) even at high velocities. At small impact parameters, however, Eq. (24) is better than Eq. (23) (Fig. 5). For instance, the LZS result in Fig. 5 shows an improper small peak at small impact parameter. The failure of the LZS formula at small ρ is more remarkable in the case of Coulombic trajectory in which a kinematical sharp peak appears at small ρ.[11,24] Equation (23) fails to reproduce this peak. This is because the rotational coupling $V_{\rm rot}$ varies rapidly at small R compared to the energy difference $\Delta\epsilon$, and a transition mechanism in the close (small ρ) collisions becomes that of the perturbed symmetric resonance. In case of large impact-parameter collisions, however, a variation of $V_{\rm rot}$ with respect to R becomes smaller compared to that of $\Delta\epsilon$, and Eq. (24) overestimates the transition probabilities. Figure 6 demonstrates the localizability of the transitions in the dynamical-potential representation.

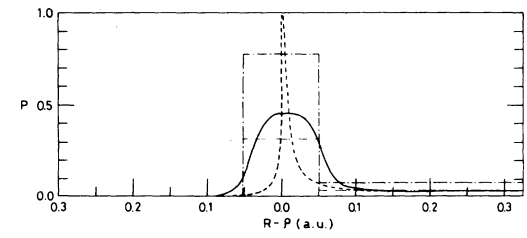

FIG. 6. Transition probabilities vs internuclear distance [model (30), $v=0.5$, $\rho=0.01$]. $-\cdots-\cdots-$: RZ approximation based on the assumption of a localized transition at $R=\mathrm{Re}(R_*)$. The meanings of other curves are the same as Fig. 3.

C. No curve crossing—case(c)

The simplest, but the most typical case of $\Delta\epsilon=$const is employed. The model can be scaled with use of reduced velocity $\tilde{v}\equiv v/\Delta\epsilon$. The angular momentum matrix element V_0 is assumed to be 0.5 a.u. The results are shown in Figs. 7–9. As is expected, Eq. (24) makes a good approximation.

V. PATH-INTEGRAL APPROACH TO A THREE-STATE PROBLEM

As an example of a three-state problem to test the applicability of the theory developed in Sec. III combined with the path-integral formulation of the scattering matrix, we have chosen a system shown in Fig. 10 which imitates a vacancy migration from the $2p$ shell to the $1s$ or the $2s$ shell in the Ne^+-Ne system.[22] There are two rotational couplings: one between the $1\pi_u$ (ϵ_1) and $2\sigma_u$ (ϵ_2) states, and the other between the $1\pi_u$ (ϵ_1) and $1\sigma_u$ (ϵ_3) states. The model potentials employed are as follows [see Eqs. (29) and (30)]:

$$\begin{aligned}
&\Delta\epsilon_{12}=\epsilon_1-\epsilon_2=2.71(1/R_x-1/R) \quad R_x=1.5\\
&\Delta\epsilon_{13}=536.9R^2,\\
&V_{12}=-V_0^{(12)}v\rho/R^2, \quad V_0^{(12)}=0.71\\
&V_{13}=-V_0^{(13)}v\rho/R^2, \quad V_0^{(13)}=1.0.
\end{aligned} \tag{31}$$

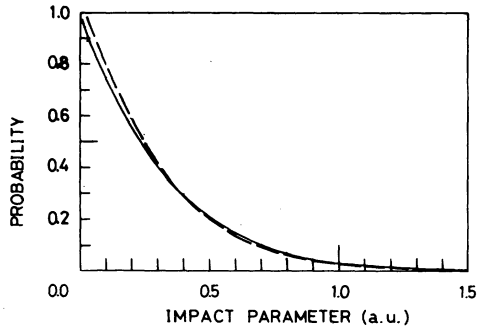

FIG. 7. The impact-parameter dependence of the transiton probabilities (const $\Delta\epsilon$ and $v/\Delta\epsilon=0.5$). —— : RZ approximation [Eq. (24)], — — — : exact numerical calculation.

The dynamical-potential energies $E_1 \sim E_3$ obtained from Eqs. (31) are

$$E_1 = \tfrac{1}{3}(\epsilon_1+\epsilon_2+\epsilon_3)+\alpha^{1/3}+\beta^{1/3},$$
$$E_2 = \tfrac{1}{3}(\epsilon_1+\epsilon_2+\epsilon_3)-\tfrac{1}{2}(\alpha^{1/3}+\beta^{1/3})-\frac{\sqrt{3}}{2}i(\alpha^{1/3}-\beta^{1/3}), \tag{32}$$
$$E_3 = \tfrac{1}{3}(\epsilon_1+\epsilon_2+\epsilon_3)-\tfrac{1}{2}(\alpha^{1/3}+\beta^{1/3})+\frac{\sqrt{3}}{2}i(\alpha^{1/3}-\beta^{1/3}),$$

where

$$\left.\begin{matrix}\alpha\\ \beta\end{matrix}\right\} = \tfrac{1}{2}[-q \pm (q^2+4p^3)^{1/2}], \tag{33}$$

$$p = -\frac{1}{9}\left[\frac{(\Delta\epsilon_{12})^2+(\Delta\epsilon_{23})^2+(\Delta\epsilon_{31})^2}{2}+3V_{12}^2+3V_{13}^2\right], \tag{34}$$

and

$$q = \tfrac{-1}{27}[(\Delta\epsilon_{12})^2(\Delta\epsilon_{23}-\Delta\epsilon_{31})+(\Delta\epsilon_{23})^2(\Delta\epsilon_{31}-\Delta\epsilon_{12})+(\Delta\epsilon_{31})^2(\Delta\epsilon_{12}-\Delta\epsilon_{23})+9(\Delta\epsilon_{12}-\Delta\epsilon_{23})V_{13}^2$$
$$+9(\Delta\epsilon_{23}-\Delta\epsilon_{31})V_{12}^2]. \tag{35}$$

Here the method of Cardano was used to solve a third-order algebraic equation. The dynamical-potential energy differences ΔE_{12} and ΔE_{13} are shown in Fig. 11.

According to the path-integral formalism the probabilities for the transitions $1\to2$ and $1\to3$ can be expressed as

$$P_{1\to2} = 4p_A(1-p_A)\left[(1-p_B)\sin^2\left[\frac{1}{v}\int_0^{x_A}\Delta E_{12}dz+\sigma_2^A+\phi_S^A-\phi_s^B+\tfrac{1}{2}\tau^B\right]+p_B^2\sin^2\left[\frac{1}{v}\int_0^{x_B}\Delta E_{23}dz+\sigma_2^B+\phi_S^B\right]\right.$$
$$+p_B\sin\left[\frac{1}{v}\int_0^{x_A}\Delta E_{12}dz+\sigma_2^A+\phi_S^A-\phi_S^B+\tfrac{1}{2}\tau^B\right]$$
$$\left.\times\sin\left[\frac{2}{v}\int_0^{x_B}\Delta E_{23}dz+\frac{1}{v}\int_0^{x_A}\Delta E_{12}dz+\sigma_2^A+\phi_S^A+2\sigma_2^B+\phi_S^B+\tfrac{1}{2}\tau^B\right]\right], \tag{36}$$

and

$$P_{1\to3} = 4p_Ap_B(1-p_B)\sin^2\left[\frac{1}{v}\int_0^{x_B}\Delta E_{23}dz+\sigma_2^B+\phi_S^B\right], \tag{37}$$

where

$$z_*^{A,B} = x_{A,B}+iy_{A,B}, \tag{38a}$$

$$\sigma_2^{A,B} = -\frac{1}{v}\int_0^{y_{A,B}}\mathrm{Im}\Delta E_{12,23}(x=x_{A,B},y)dy, \tag{38b}$$

$$p_A = \exp(-2\delta_A), \tag{38c}$$

$$p_B = \exp(-2\delta_B), \tag{38d}$$

$$\delta_{A,B} = \frac{1}{v}\mathrm{Im}\int_0^{z_*^{A,B}}\Delta E_{12,23}dz, \tag{38e}$$

$$\phi_S^{A,B} = \frac{\pi}{4}-\frac{1}{\pi}\delta_{A,B}+\frac{1}{\pi}\delta_{A,B}\ln\frac{\delta_{A,B}}{\pi}-\arg\Gamma\left[1+\frac{i}{\pi}\delta_{A,B}\right], \tag{38f}$$

and

$$\tau^B = \tfrac{1}{2}\tan^{-1}\frac{\pi}{2\delta_B}$$
$$+\frac{\delta_B}{\pi}\ln\left\{\frac{\delta_B}{\pi}\Big/\left[\frac{1}{4}+\left[\frac{\delta_B}{\pi}\right]^2\right]^{1/2}\right\}. \tag{38g}$$

Numerical results in comparison with the exact ones are shown in Figs. 12–15. These figures clearly indicate the usefulness of the theory. Transitions between $1\pi_u$ and $1\sigma_u$ occur dominantly at smaller impact parameters compared to the transitions between $1\pi_u$ and $2\sigma_u$. Since p_B is small at

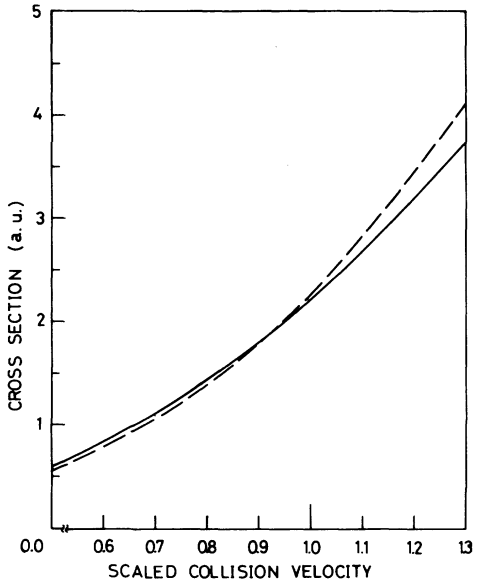

FIG. 8. Total cross sections as a function of collision velocity (const $\Delta\epsilon$). See the caption of Fig. 7.

those impact parameters which contribute much to the transitions between $1\pi_u$ and $2\sigma_u$, the main contribution to $P_{1\to2}$ comes from the first term of Eq. (36). Similarly, p_A is almost equal to unity at those impact parameters for which the transitions between $1\pi_u$ and $1\sigma_u$ occur dominantly, and $P_{1\to3}$ is expected to be nearly equal to the probability in the two-state problem.

Figures 12—15 also indicate an interesting phenomenon of a catalysis effect of the $2\sigma_u$ state on the transition from $1\pi_u$ to $1\sigma_u$. The dotted lines in the figures represent the exact results in the relevant two-state approximations. The transition $1\to2$ is not affected at all by an inclusion of the $1\sigma_u$ state. The transition $1\to3$, however, is enhanced a lot by an inclusion of the $2\sigma_u$ state. This enhancement was confirmed not to be affected

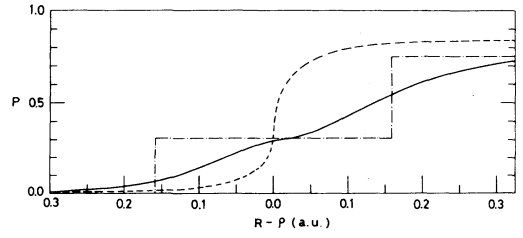

FIG. 9. Transition probabilities vs internuclear distance (const $\Delta\epsilon$, $v=0.5$, $\rho=0.1$). —·—·—·: RZ approximation. The meanings of other curves are the same as Fig. 3.

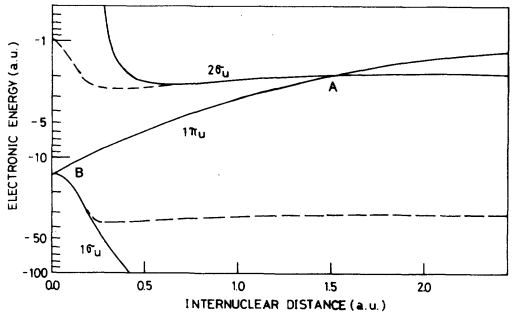

FIG. 10. The electronic energy diagram of the $1\sigma_u$, $1\pi_u$, and $2\sigma_u$ states of the Ne^+-Ne system. — — —: Energies calculated from the variable screening model (Ref. 22), ——: model potentials used in this paper.

by changing the location of the crossing point $R=R_x$, but to diminish with smaller $V_0^{(12)}$. Since p_A cannot be larger than unity, this phenomenon seems to give us a puzzle [see Eq. (37)]. It should be noted, however, that the energy difference ΔE_{23} includes the influence of the rotational coupling V_{12} between the $1\pi_u$ and $2\sigma_u$ states. That is, the deformation of ΔE_{23} at $R\sim R_B$ due to the coupling V_{12} can explain the catalysis effect of the $2\sigma_u$ state on the transition $1\to3$ (see Figs. 11, 14, and 15). It is true that the energy difference ΔE_{12} at $R\sim R_A$ includes the effect of the coupling V_{13}; but this effect is negligible, since the rotational coupling decays as R increases. This interesting phenomenon leads to the following conclusion: Rotational couplings not directly associated with the transitions we are interested in, may affect these transitions if the avoided crossing points corresponding to the transitions are located at small R, and if the angular momentum matrix element V_0 of the couplings are not very small there. This phenomenon can be reproduced by our theory based on the dynamical states obtained by diagonalizing the matrix $(\underline{\epsilon}+\underline{V}_{\rm rot})$ at one time [see Eq. (22)].

VI. DISCUSSION

The nonadiabatic radial coupling is known to be well localized at an avoided crossing point in the ordinary adiabatic-state representation. The nonadiabatic rotational coupling, on the other hand, is not localized at all, since it is proportional to R^{-2}. Because of this fact an analytical solution of a many-state collision problem involving rotational couplings has been left untractable so far. The dynamical-state representation discussed in this pa-

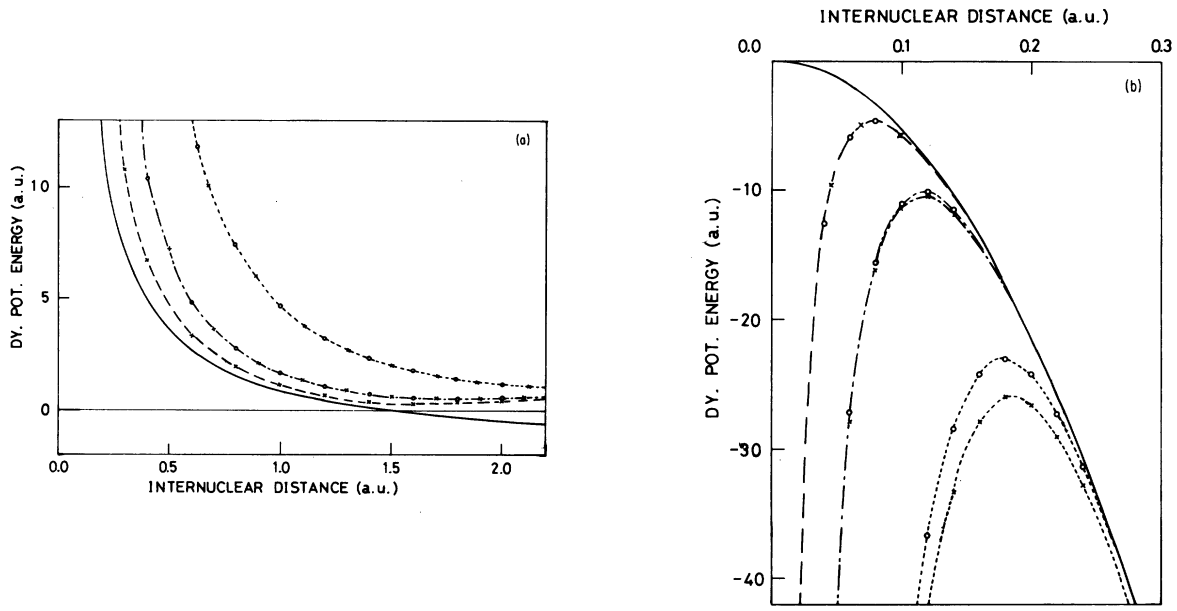

FIG. 11. Dynamical potential energy difference [Eqs. (32)]. (a) $\Delta E_{12}=E_1-E_2$; $E_1\rightarrow\epsilon(1\pi_u)$, $E_2\rightarrow\epsilon(2\sigma_u)$ $(R\rightarrow\infty)$. —— : $\Delta\epsilon_{12}=\epsilon(2\sigma_u)-\epsilon(1\pi_u)$, — — — : $v\rho=0.51$, — · — · —: $v\rho=1.03$, - - -: $v\rho=3.24$. The crosses represent the dynamical states obtained with $V_0^{(13)}$ put equal to zero. The circles are the dynamical states obtained by diagonalizing the 3×3 matrix [Eqs. (32)]. (b) $\Delta E_{32}=-\Delta E_{23}=E_3-E_2$; $E_3\rightarrow\epsilon(1\sigma_u)$ $(R\rightarrow\infty)$. —— : $\Delta\epsilon_{32}=-\epsilon(1\pi_u)+\epsilon(1\sigma_u)$, — — — : $v\rho=0.01$, — · — · —: $v\rho=0.05$, - - -: $v\rho=0.31$. The crosses represent the dynamical states obtained with $V_0^{(12)}$ put equal to zero. The circles are the dynamical states obtained by diagonalizing the 3×3 matrix [Eqs. (32)].

per localizes even a rotationally induced transition at a new avoided crossing point; and enables us to treat a many-state collision problem involving both radial and rotational couplings by the classical scattering matrix theory based on the path-integral formulation of quantum mechanics.

An interesting catalytic phenomenon such as the one discussed in Sec. V is expected to take place generally in a many-state collision problem involving rotational couplings, if the relevant transitions predominantly occur at small internuclear distances. In order to reproduce the phenomenon it is necessary to diagonalize a multidimensional matrix $(\underline{\epsilon}+\underline{V}_{\rm rot})$ at one time. If a transition occurs at large internuclear distances, however, a catalysis effect of other states can be negligible and it may be all right to diagonalize locally the relevant two-dimensional matrix corresponding to the transitions.

In the model calculations of Sec. V we assumed

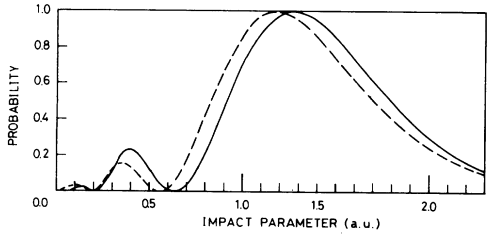

FIG. 12. The impact-parameter dependence of the transition probabilities $P_{1\rightarrow2}$ $(1\pi_u\rightarrow2\sigma_u)$ at $v=0.9$. —— : Path-integral approximation [Eq. (36)], — — — : exact numerical calculation. The two-state results are practically the same as these.

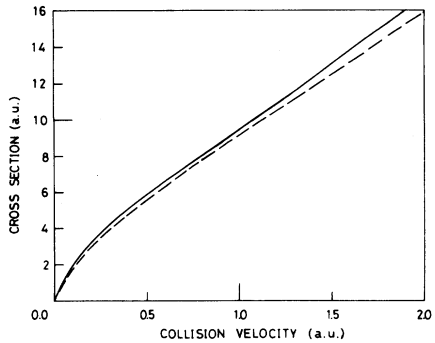

FIG. 13. The total cross sections $\sigma_{1\rightarrow2}$ $(1\pi_u\rightarrow2\sigma_u)$ as a function of collision velocity (see the caption of Fig. 12).

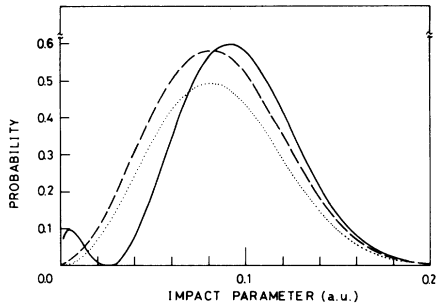

FIG. 14. The impact-parameter dependence of the transition probability $P_{1\to3}$ ($1\pi_u \to 1\sigma_u$) at $v=0.9$. —— : Path-integral approximation [Eq. (37)], — — — : exact numerical calculation (three-state), ...: exact numerical calculation (two-state).

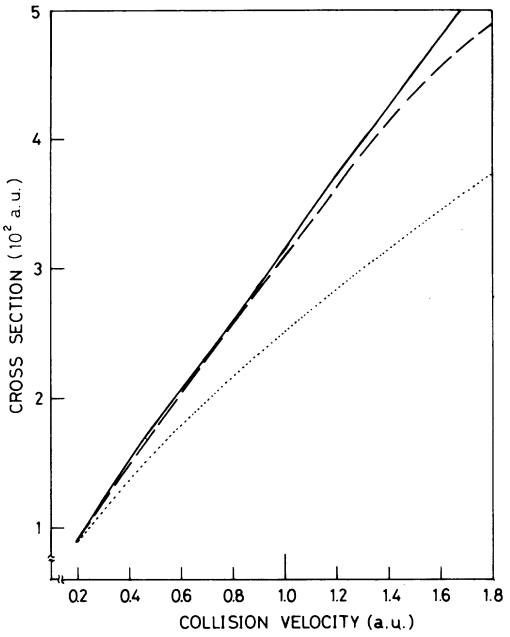

FIG. 15. Total cross sections $\sigma_{1\to3}$ ($1\pi_u \to 1\sigma_u$) as a function of collision velocity (see the caption of Fig. 14).

$V_0^{(12)}$ to be constant. This is of course an approximation to the coupling in the real Ne^+-Ne system, and probably causes an overestimation of the catalysis effect of the $2\sigma_u$ state. It is, however, necessary to reinvestigate more carefully the transition from $1\pi_u$ to $1\sigma_u$ by using accurate information on potential energies and couplings for the Ne^+-Ne system. Apart from the Ne^+-Ne problem, on the other hand, $V_0^{(12)}$ does not necessarily vanish at $R=0$ all the time. In such cases $[V_0^{(12)}(R=0)\neq 0]$ the catalysis effect is expected to occur remarkably as in the present model calculations. Another interesting problem to be investigated by the theory developed in this paper is

$$\mathrm{Li}^+ + \mathrm{Na} \to \begin{cases} \mathrm{Li}^*(2p) + \mathrm{Na}^+ \\ \mathrm{Li}(2s) + \mathrm{Na}^+ \end{cases},$$

where the Li^+-Na and Li^*-Na^+ states couple to each other rotationally, and the Li^+-Na and Li-Na^+ states couple radially by the Demkov-type mechanism.[25,26]

In this paper we have employed the semiclassical impact-parameter method for simplicity. Strictly speaking, however, a transition through rotational coupling induces a change of the angular momentum of the relative motion of heavy particles, since the electronic angular momentum changes by unity in the transition. In the semiclassical impact-parameter treatment, which is not bad in the case of heavy-particle collisions, this change is neglected and the angular momentum quantum number is replaced by $M v\rho/\hbar$, where M is the reduced mass of the collision system. In order to look into the detailed quantum effects in the transitions, we should, of course, rely on the exact quantum-mechanical treatment.[21,27]

This work was supported by a Grant in Aid for Scientific Research from the Ministry of Education of Japan.

*Present address: Institute for Molecular Science, Myodaiji, Okazaki 444, Japan.

[1]H. Nakamura, J. Phys. Soc. Jpn. 26, 1473 (1969).
[2]H. Nakamura, Chem. Phys. 10, 271 (1975).
[3]See, for instance, K. S. Lam and T. F. George, *Semiclassical Methods in Molecular Scattering and Spectroscopy*, edited by M. S. Child (Reidel, Boston, 1980), pp. 179–261.
[4]U. Fano, Phys. Rev. A 2, 353 (1970).
[5]Ch. Jungen and O. Atabek, J. Chem. Phys. 66, 5584 (1977).
[6]M. Raoult and Ch. Jungen, J. Chem. Phys. 74, 3388 (1981).
[7]H. Takagi and H. Nakamura, J. Chem. Phys. 74, 5808 (1981).
[8]A. Giusti, J. Phys. B 13, 3867 (1980).

[9]C. Greene, U. Fano, and G. Strinati, Phys. Rev. A 19, 1485 (1979).
[10]See, for instance, Q. C. Kessel and B. Fastrup, Case Stud. At. Phys. 3, 137 (1973).
[11]H. Nakamura and M. Namiki, J. Phys. Soc. Jpn. 49, 843 (1980).
[12]D. S. F. Crothers, Adv. Phys. 20, 405 (1971).
[13]See, for instance, W. H. Miller, Adv. Chem. Phys. 30, 77 (1975).
[14]Yu. N. Demkov, V. N. Ostrovskii, and E. A. Solov'ev, Phys. Rev. A 18, 2089 (1978).
[15]Yu. N. Demkov, C. V. Kunasz, and V. N. Ostrovskii, Phys. Rev. A 18, 2097 (1978).
[16]S. C. Miller and R. H. Good, Phys. Rev. 91, 174 (1953).
[17]M. S. Child, Mol. Phys. 20, 171 (1971).
[18]D. S. F. Crothers, J. Phys. B 9, 635 (1976); A 5, 1680 (1972).
[19]W. Fritsch and U. Wille, J. Phys. B 11, L43 (1978).
[20]M. Namiki, H. Yagisawa, and H. Nakamura, J. Phys. B 13, 743 (1980).
[21]F. T. Smith, Phys. Rev. 179, 111 (1969).
[22]W. Fritsch and U. Wille, J. Phys. B 11, 4019 (1978).
[23]J. S. Briggs and J. H. Macek, J. Phys. B 6, 982 (1973).
[24]D. S. F. Crothers and J. G. Hughes, J. Phys. B 12, 3063 (1979).
[25]F. von Busch, J. Hormes, and H. D. Liesen, Chem. Phys. Lett. 34, 244 (1975).
[26]T. Okamoto, Y. Sato, N. Shimakura, and H. Inouye, J. Phys. B 14, 2379 (1981).
[27]W. R. Thorson, J. Chem. Phys. 34, 1744 (1961).